



A02-13590

AIAA-2002-0487

Hall Thruster Far Field Plume Modeling
And Comparison to Express Flight Data

I. D. Boyd

University of Michigan

Ann Arbor, MI 48109.

**40th AIAA Aerospace Sciences
Meeting & Exhibit**
14-17 January 2002 / Reno, NV

AIAA PAPER 2002-0487

**Presented at AIAA 40th Aerospace Sciences Meeting
Reno, NV, January 2002**

**HALL THRUSTER FAR FIELD PLUME MODELING
AND COMPARISON TO EXPRESS FLIGHT DATA**

Iain D. Boyd*

University of Michigan, Ann Arbor, MI 48109

Abstract

Hall thrusters are an attractive form of electric propulsion that are being developed and implemented to replace chemical systems for many on orbit propulsion tasks on communications satellites. One concern in the use of these devices is the possible damage their plumes may cause to the host spacecraft. Computer models of Hall thruster plumes play an important role in integration of these devices onto spacecraft as the space environment is not easily reproduced in ground testing facilities. In this paper, a hybrid particle-fluid model of a Hall thruster plume is applied to model the SPT-100 thrusters used on the Russian Express satellites. The emphasis of the paper is on making assessment of the model through direct comparison with measurements of ion current density and ion energy distributions taken on board Express spacecraft. These data challenge the model in two ways. First, they represent the first set of Hall thruster plume measurements obtained in space, whereas the computer models have been developed based on measurements taken in ground-based facilities. Second, most of the data measurement locations are several meters from the thruster requiring careful consideration of the plume far-field.

Introduction

Hall thrusters are under development in several countries including the United States, Russia, Japan, and France. These electric propulsion devices typically offer a specific impulse of about 1,600 sec and a thrust of about 80 mN. These characteristics make them ideally suited for spacecraft orbit maintenance tasks such as north-south station keeping. Under typical operating conditions, at a power level of about 1.5 kW, a voltage of 300 V is applied between an external cathode and an annular anode. The electrons emitted from the cathode ionize the xenon propellant efficiently aided by magnetic confinement within an annular acceleration channel (creating an azimuthal Hall current). The ions are accelerated in the imposed electric field to velocities on the order of 17 km/sec. New classes of Hall thrusters are being developed at low power (100 W) for use on micro-spacecraft, and at high power (25 kW) for spacecraft orbit-raising.

As with any spacecraft propulsion device (chemical or electric), computer modeling is used to assess any interactions between the plume of the thruster and the host spacecraft. In the case of Hall thrusters,

* Associate Professor. Department of Aerospace Engineering. Senior Member AIAA

there are three particular spacecraft integration issues: (1) the divergence angle of these devices is relatively large (about 60 deg) leading to the possibility of direct impingement of high energy propellant ions onto spacecraft surfaces that may result in sputtering and degradation of material properties. Material sputtered from spacecraft surfaces in this way may ultimately become deposited on other spacecraft surfaces such as solar cells, causing further problems; (2) back flow impingement of ions caused by formation of a charge exchange plasma; and (3) the high energy ions created inside the thruster cause significant erosion of the walls of the acceleration channel (usually made of metal or a ceramic such as boron nitride) and the erosion products may expand out from the thruster and become deposited on spacecraft surfaces.

A number of Hall thruster plume models have been developed and these are reviewed in a recent article by Boyd.¹ These models have been assessed against detailed experimental data taken in the plumes of a variety of Hall thrusters in ground-based vacuum chambers. For a 1.5 kW class Hall thruster, the lowest background pressure that can be obtained in vacuum chambers is about 10^{-6} torr, which corresponds to an orbital altitude of about 185 km. Clearly, this represents a pressure that is orders of magnitude higher than that encountered in the operation of Hall thrusters in geostationary earth orbit (GEO). Another limitation of vacuum chambers concerns their size. Most Hall thruster plume measurements have been taken such that the maximum distance from the thruster that was probed was about 1 m.

The primary objective of this article is to assess a state-of-the-art Hall thruster plume model in terms of its predictions for realistic space conditions of the far field of the plume. The assessment is made possible by the recent, in-orbit, plume measurements of SPT-100 Hall thrusters taken on board the Russian Express spacecraft.² The outline of the paper is as follows. First, an outline of the Express spacecraft and the plume measurements is provided. Then, a description is given of the hybrid particle-fluid plume model employed in this study. Results consisting of comparisons between measured and computed data for ion current density and ion energy distributions are then presented and discussed. The sensitivity of the model predictions to various physical modeling assumptions and boundary conditions is considered. The paper closes with some conclusions and suggestions for further work.

Express Flight Data

A complete description of the two Russian Express-A satellites and the flight data collection program are provided by Manzella et al.² The thrusters employed on the spacecraft were SPT-100 models with a nominal thrust level of about 82 mN while operating at a discharge current of 4.5 Amp and a total flow rate (anode plus cathode) of 5.3 mg/sec. In some ways, the use of SPT-100 thrusters for the first recording of in-orbit plume data is most appropriate as this thruster has received the most attention in terms of both laboratory studies^{3,4,5,6,7} and computational analysis.^{7,8,9} A variety of sensors were employed on board the two spacecraft to characterize the effects of firing the Hall thrusters on the spacecraft operation and environment. These include electric field sensors, Faraday probes to measure ion current density, retarding potential analyzers (RPA's) to measure ion current and ion energy, and pressure sensors. In addition, disturbance torques on the spacecraft imparted by the Hall thruster plumes were recorded.

From all of the above, the present study focuses on the RPA data for ion current density and ion energy distributions. This is in part due to the overlap with ground-based measurements of these properties, the relatively good apparent fidelity of these data, and the lack of post-flight reduction of much of the other data. The locations where RPA data was measured are plotted in Fig. 1 with respect to an origin in the thruster exit plane on the thruster centerline. The variation in location is due to the firing of eight different thrusters and the fact that some of the sensors could be moved. Note that some of the sensors were as much as 8.8 m away from the thruster which is well in to the far-field region of the plume.

Hall Thruster Plume Model

To understand the type of numerical approach required to accurately model Hall thruster plumes, it is informative to consider some of the basic physical characteristics of the flow exiting from the thruster. In Table 1, typical values of some of the pertinent properties are listed at the thruster exit for the SPT-100. For these plasma densities, the Debye length is very small, on the order of 10^{-5} m which indicates that the plume is charge neutral for a relatively large distance away from the thruster. At the same time, the collision mean free paths are very large, on the order of 1 m. These fundamental physical properties of the plume suggest that a kinetic approach is necessary that simulates both plasma and collision effects.

In this study, a hybrid particle-fluid model is employed. The Particle In Cell method (PIC)¹⁰ is employed to model the plasma dynamics, and the direct simulation Monte Carlo method (DSMC)¹¹ is used to simulate the collision dynamics. In the following, these models are briefly outlined.

Plasma Dynamics

The first efforts to use a combination of the PIC and DSMC methods to model the plumes of Hall thrusters were made by Oh et al.⁷ and this approach has formed the basis for subsequent work.^{8,12} In general, the PIC method accelerates charged particles through applied and self-generated electric fields in a self-consistent manner. In Ref. 7, based on the plasma jet physical properties, the ions are modeled as particles and the electrons as a fluid. The plasma potential is obtained by assuming quasi-neutrality, which allows the ion density to represent the electron density. By further assuming that the electrons are isothermal, collisionless, and un-magnetized, and that their pressure obeys the ideal gas law, $p = nkT$, the Boltzmann relation is obtained:

$$\phi - \phi^* = \frac{kT}{e} \ln \left(\frac{n}{n^*} \right) \quad (1)$$

where n is the electron number density, $*$ indicates a reference state, ϕ is the plasma potential, k is Boltzmann's constant, T is the constant electron temperature, and e is the electron charge. The potential is differentiated spatially to obtain the electric fields.

There are several limitations of this approach. Firstly, experimental evidence^{3,5} indicates that there is variation of the electron temperature in Hall thruster plumes. The variation occurs mainly in the near-field

of the plume. At the thruster exit the electron temperature can be as high as 10 eV⁵ and in the far field typical values are 1 to 2 eV.³ This creates a difficulty in the choice of T to be used in Eq. (1). A further difficulty with application of the Boltzmann relation to Hall thruster plumes is the possible effects of the magnetic field. The combination of permanent and electro-magnets employed in Hall thrusters are designed to provide optimum device performance. However, some of the magnetic field may leak out into the plume of the thruster. The amount of this leakage will depend strongly on the Hall thruster type and configuration.

Despite these limitations, the simple Boltzmann relation is widely used and has produced remarkably good agreement with a number of different plume properties measured in vacuum chambers, see Ref. 1 for examples. This approach therefore forms the baseline model for the present study. An alternative approach sometimes employed in plasmadynamics is to assume that the electrons behave adiabatically in which the pressure, density, and temperature are related by:

$$\frac{p}{p^*} = \left(\frac{n}{n^*}\right)^\gamma = \left(\frac{T}{T^*}\right)^{\frac{\gamma}{\gamma-1}} \quad (2)$$

where γ is the ratio of specific heats, and * again indicates a reference state. Thus, changes in the electron temperature are related to changes in the electron density. Substitution of Eq. (2) into the electron momentum equation, assuming collisionless, un-magnetized electrons gives:

$$\phi - \phi^* = \frac{kT^*}{e} \frac{\gamma}{\gamma-1} \left[\left(\frac{n}{n^*}\right)^{\gamma-1} - 1 \right] \quad (3)$$

Results obtained with this adiabatic approach are compared to the baseline solutions obtained with the Boltzmann relation.

Collision Dynamics

The DSMC method uses particles to simulate collision effects in rarefied gas flows by collecting groups of particles into cells which have sizes of the order of a mean free path. Pairs of these particles are then selected at random and a collision probability is evaluated for each pair that is proportional to the product of the pair's relative velocity and collision cross section. The probability is compared with a random number to determine if that collision occurs. If so, some form of collision dynamics is performed to alter the properties of the colliding particles.

There are two basic classes of collisions that are important in Hall thruster plumes: (1) elastic (momentum exchange); and (2) charge exchange. At first glance, based on the low number densities at the thruster exit, it appears that collisions are unimportant in Hall thruster plumes. However, it will be found in the discussion of results, that these collisions have a profound effect on the Hall thruster plume structure even though the mean free path for all collisions is large. Two different approaches to modeling the ion-atom collision processes are followed. In the first, simple scattering laws are combined with analytical models and experimental measurements for the cross sections. In the second approach, the scattering is determined by detailed calculations.

Simple Model

Elastic collisions involve only exchange of momentum between the participating particles. For the systems of interest here, this may involve atom–atom or atom-ion collisions. For atom–atom collisions, the Variable Hard Sphere (VHS)¹¹ collision model is employed. For xenon, the collision cross section is:

$$\sigma_{EL}(Xe, Xe) = \frac{2.12 \times 10^{-18}}{g^{2\omega}} \text{m}^2 \quad (4)$$

where g is the relative velocity, and $\omega=0.12$ is related to the viscosity temperature exponent. For atom–ion elastic interactions, the following cross section of Dalgarno et al.¹³ is employed:

$$\sigma_{EL}(Xe, Xe^+) = \frac{6.42 \times 10^{-16}}{g} \text{m}^2 \quad (5)$$

The model of Ref. 13 predicts that the elastic cross section for interaction between an atom and a doubly charged ion is twice that for an atom and a singly charged ion. It should be noted that the model of Ref. 13 employs a polarization potential and therefore is only valid for low energy (a few eV) collisions. In all elastic interactions, the collision dynamics is modeled using isotropic scattering together with conservation of linear momentum and energy to determine the post-collision velocities of the colliding particles.¹¹

Charge exchange concerns the transfer of one or more electrons between an atom and an ion. This is a long-range interaction that involves a relatively large cross section in comparison to an elastic interaction. This is an important mechanism in Hall thruster plumes because at the thruster exit plane, the atoms and ions have velocities that differ by almost two orders of magnitude (see Table 1). While the ions have been accelerated electrostatically, the atoms remain at thermal speeds. Thus, charge exchange leads to a slow ion and a fast atom. The slow ion is much more responsive to the electric fields set up in the plume and are easily pulled behind the thruster into the back flow region. Thus, the so-called charge exchange plasma is formed near the thruster exit. It is because we need to model the charge exchange behavior accurately that we go to the trouble of using the DSMC technique.

For singly charged ions, the following cross section measured by Miller et al.¹⁴ is used:

$$\sigma_{CEX}(Xe, Xe^+) = (-23.30 \log_{10}(g) + 142.21) \times 0.8423 \times 10^{-20} \text{m}^2 \quad (6)$$

Also reported in Ref. 14 are charge exchange cross sections for the interaction where a doubly charged ion transfers two electrons from an atom. These cross sections are a factor of two lower than the values for the singly charged ions.

In all charge exchange interactions, the collision dynamics assumes that there is no transfer of momentum accompanying the transfer of the electron(s). This assumption is based on the premise that these interactions are at long range.

Detailed Model

In this approach, the VHS model for Xe-Xe collisions is again employed along with isotropic scattering. The charge exchange collisions employ the same measured cross sections, but scattering is modeled using

data computed by Dressler and reported in Ref. 15. The differential cross sections computed by Dressler are shown in Fig. 2 as a function of scattering angle. These results indicate (as expected) that the majority of charge exchange interactions involve very low angle scattering. However, the calculations do not distinguish between charge exchange and momentum exchange and so the same scattering data is employed for atom-ion momentum exchange interactions. The cross section employed for these elastic collisions is the same as that for charge exchange that is again based on the experimental measurements of Ref. 14.

Boundary Conditions

For PIC-DSMC computations of Hall thruster plumes, boundary conditions must be specified at several locations: (1) at the thruster exit; (2) along the outer edges of the computational domain; and (3) along any solid surfaces in the computational domain.

Several macroscopic properties of the plasma exiting the Hall thruster acceleration channel are required for PIC-DSMC computations. Specifically, the plasma potential, the electron temperature, and for each of the particle species we require the number density, velocity, and temperature. In the real device, these properties will vary spatially across the annular face of the thruster exit plane, but also in many operating modes of the thruster these quantities vary in time. In general, the approach to determining these properties is a mixture of analysis and estimation. By assuming ion and neutral temperatures (typically 4 eV and 1,000 K, respectively) and using measured properties such as thrust, mass flow rate, and current, it is possible to determine the species number densities and velocities. This approach gives uniform profiles of all properties across the exit plane. Generally, a small half-angle is imposed at the thruster exit plane to provide a variation in the velocity vector. An alternative approach considered here uses output from a two-dimensional PIC-MCC (Monte Carlo Collision) model of the acceleration channel¹⁶ as input to a PIC-DSMC plume computation.

Both field and particle boundary conditions are required at the outer edges of the computational domain. The usual field conditions employed simply set the electric fields normal to the boundary edges equal to zero. For plume expansion into vacuum, the particle boundary condition is to remove from the computation any particle crossing the domain edge.

In all configurations, the solid exterior walls of the thruster must be included in the computation. In the present study, the potential of the walls is set to zero. Any ions colliding with the thruster walls are neutralized. Both atoms and neutralized ions are scattered back into the flow field from the surface of the thruster wall assuming diffuse reflection.

Results

The Hall thruster plume model described above is assessed by making direct comparison with ion current and ion energy distributions measured on-board the Express spacecraft. The baseline simulation is performed as follows: (1) at the thruster exit, the densities and temperatures are assumed to be radially uniform, the velocities are based on a divergence angle of 15 deg., an ion temperature of 4 eV is assumed,

and the densities and velocities are obtained from the mass flow rate and integrated ion current; (2) the Boltzmann relation is used with a fixed electron temperature of 3 eV; (3) the “detailed” collision model is employed. The sensitivity of the model predictions to these assumptions is considered.

The computational domain extends more than 10 m axially from the thruster exit and 10 m radially from the thruster centerline to cover all of the Express probe locations. This is achieved using a mesh containing 190 by 175 non-uniform, rectangular cells. In a typical computation approximately 4 million particles are employed with about 60% representing ions (both single and double charged). The neutral atom flow is first allowed to reach a steady state by using a large time step. The ions are then subsequently introduced with a time step of about 10^{-7} sec. The computations reach a steady state for the ions after about 5,000 iterations and solutions are then averaged over a further 10,000 iterations. The total computation time is about 24 hours on a personal computer. In Figs. 3 and 4, contours are shown of the ion and neutral atom number densities, respectively. These show that the two populations follow quite different plume expansion dynamics. The charge exchange plasma formed vertically above the thruster exit plane can be seen in Fig. 3.

Ion Current Density

Angular profiles of ion current density are shown in Fig. 4 in which the Express data are compared with two different profiles measured for the SPT-100 in vacuum chambers by Manzella⁴ and King.⁶ There are several important points to be noted in this plot. First, while the laboratory data were obtained at 1 m from the thruster, as shown in Fig. 1, this is not the case for the Express measurements. To try to simplify the data comparisons, the Express data are extrapolated to values at 1 m from the thruster using a $1/r^2$ relation for the decay in ion current density with distance from the thruster. The accuracy of this relation will be considered later. The figure also indicates that there is considerable spread in the Express data. In some cases, for the same angular location, there is as much as an order of magnitude variation. This illustrates the challenge in obtaining good quality plume data under in-orbit conditions. Thus, in general, it is not the aim of the modeling to agree exactly with the data, but rather the emphasis is on examining trends. Comparison of the three data sets in Fig. 5 shows the effect of the increased back-pressure found in vacuum chamber experiments. As the back pressure is decreased from the King experiment, to the Manzella experiment, to the Express flight, the ion current density profile shows a significant decay at high angles. Close to the plume axis, the Express data is consistently a factor of two to three lower than the laboratory data. It is not clear whether this difference is real or part of a systematic error in the Express measurements. As noted earlier, the development and assessment of Hall thruster plume models has been performed exclusively using laboratory data. The Express data is the first set of measurements obtained in-orbit for the plume of a Hall thruster. Figure 6 shows an example from the work of Van Gilder et al.⁸ that illustrates the levels of agreement that have been achieved between these plume models and the laboratory data for ion current density. One of the main questions to be answered in this study is whether these same models are able to predict the space-flight data.

In Fig. 7, angular profiles of ion current density are shown in which the Express data is compared to

two profiles obtained from the same baseline simulation. The Express data and a simulation profile obtained at 8.8 m from the thruster are each extrapolated using the $1/r^2$ relation to 1 m from the thruster. The second simulation profile is obtained directly at 1 m from the thruster. Comparison of the two simulation results indicates that the ion current density does not exactly scale as $1/r^2$. At 8.8 m, the ion current density extrapolated to 1 m is a little lower at small angles and has a different overall shape in comparison to the actual 1 m result. It is believed that these differences are due primarily to collision effects. If there are no collisions in the plume, then the $1/r^2$ relation should hold for ion current density. However, the few collisions that do occur tend to scatter ions away from the axis leading to a relative reduction in ion current density there. Another important aspect concerns the effects of the electric fields that also change the ion dynamics from the simple scaling law. Therefore, in most of the simulation data shown in the remainder of this study, the plume data obtained at 8.8 m and scaled using the $1/r^2$ relation is shown rather than the data obtained directly at 1 m. It is interesting to note that the 8.8 m simulation profile appears to offer better agreement to the Express data at most angles.

The effect of the fixed value of electron temperature in the simulation on the ion current density profiles is shown in Fig. 8. There is a consistent trend in which the profile becomes lower and flatter as the electron temperature increases. The value of 8 eV is chosen as this was employed in a plume model reported in Ref. 2. However, laboratory measurements of electron temperature indicate that this value is much too high except for a small region right at the thruster exit. In terms of the PIC-DSMC plume model, the value of 3 eV appears to offer the best agreement with the Express data.

The effect of the collision model on ion current density is examined next in Fig. 9. Simulation profiles obtained using the “simple” collision model at 1 m, 3.8 m, and 8.8 m from the thruster (with the latter two extrapolated to 1 m) are compared with the Express data. It is immediately clear that the “simple” collision model has a huge effect on the plume structure that grows with distance from the thruster. The most significant difference between the “simple” and “detailed” collision models is the treatment of momentum exchange collisions. Relatively speaking, the “simple” model has a smaller collision probability than the “detailed” model. However, the “simple” model assumes isotropic scattering after collision that can lead to very large changes in the properties of the ion following each collision. By comparison, the majority of momentum exchange collisions in the “detailed” model involve very small angle scattering with little change in the properties of the ion. Thus, despite its smaller total cross section, the large angle differential cross sections of the “simple” model are significantly larger than those for the “detailed” model and lead to significant scattering of the ions away from the plume centerline at large distances from the thruster.

Finally, in Fig. 10, the effects are examined on ion current density of the properties assumed at the exit of the Hall thruster. The baseline solution is compared with a simulation in which the exit profiles are obtained from a PIC-MCC simulation of the Hall thruster acceleration channel.¹⁶ The PIC-MCC simulation predicts significant variation in all the ion and neutral atom flow properties across the thruster exit (see Ref. 16 for detailed discussion). The main point here is that the profiles employed in the results labeled

“PIC-MCC” are significantly different from those employed in the other simulations. It is interesting to note, however, that the effects of these differences on the ion current density profile at 8.8 m from the thruster are quite small, with the main deviation occurring on the plume centerline where the “PIC-MCC” profile has a larger value.

Primary Beam Ion Energy Distribution

The ion energy distribution in the primary beam near to the centerline (at 7 deg.) and a distance of 3.76 m is now considered. In Fig. 11, the Express data is compared with the results of the baseline simulation. Note, in terms of plotting style, that exact agreement between the data sets would mean that the solid line employed for the model results would go through the center of the horizontal bar of each column of the histogram used for the Express data. Ion energy distributions have been measured near centerline for the SPT-100 thruster in vacuum chambers by Myers and Manzella (using an RPA),³ King (using a molecular beam mass spectrometer, MBMS),⁶ and Perot et al. (using an RPA).¹⁷ Table 2 lists the full width half maximum energy obtained in each of these experiments. Clearly, the RPA data measured in space provides the narrowest distribution and this is perhaps explained by collisional broadening present in the vacuum tank experiments. Returning to Fig. 11, in general there is good agreement although the simulation distribution is clearly broader than the measured profile. The effect of the value of electron temperature assumed in the simulation is investigated in Fig. 12. A trend is observed in which the peak of the distribution moves to higher ion energies as the electron temperature is increased. The width of the distribution is unchanged.

The effects on the simulation results of various aspects of physical modeling are shown in Fig. 13. Use of 1 eV for the ion temperature at the thruster exit leads to a narrower ion energy distribution that is closer to the Express data. Use of the “simple” collision model moves the peak of the distribution to a higher energy but does not change the width of the distribution. The movement of the distribution is assumed to occur as a result of the relatively large high-angle differential cross section for ion-atom momentum exchange used in the “simple” model. This leads to a stronger decay in ion density along the axis that in turn leads to stronger electric fields acting along the axis as a result of the Boltzmann relation. Although not shown here, it is found that use of the adiabatic model for the electrons gives an ion energy distribution that is identical to that obtained with the baseline simulation.

Finally, in Fig. 14, the energy distribution are shown that are obtained using the PIC-MCC results at the thruster exit. This simulation shows good agreement with the width and shape of the measured distribution.

Charge Exchange Ion Energy Distribution

The ion energy distribution obtained at the large angle of 77 deg (see Fig. 1) is now considered. This location is of interest since it is characterized primarily by charge exchange ions. Very few beam ions are expected to exit the Hall thruster at such large angles. In Fig. 15, the Express data are compared with the results from the baseline simulation. Figure 15 illustrates a high energy structure measured on-board the

Express spacecraft that extends up to values associated with primary beam ions of about 260 eV. These high energies are not simulated by the model, although the peak of the distribution at about 28 eV is well predicted. King⁶ measured the ion energy distribution function at 1 m from the SPT-100 from centerline to well behind the thruster including data collection at 80 deg.. Unfortunately, the data at ± 80 deg. are far from identical and the MBMS diagnostic was not designed to detect the low energy ions measured by the Express RPA instrument.

The sensitivity of the model results to the electron temperature is investigated in Fig. 16. Increasing the electron temperature leads to the movement of the location of the peak of the distribution to higher ion energy. The value of 3 eV employed in the baseline simulation provides the best agreement with the Express data.

Next, the effects of changing various aspects of the physical modeling employed in the simulations are considered. Specifically, the “simple” collision model and the adiabatic electron model are each employed in separate simulations. Figure 17 shows that the adiabatic model leads to a broader ion energy distribution with a peak at a lower ion energy. This indicates a smaller degree of ion acceleration with this model and is explained by the fact that for large regions of the plume, the adiabatic model predicts electron temperatures that are significantly lower than 1 eV. The effect of the “simple” collision model on the charge exchange plasma is to move the peak of the distribution to a significantly higher ion energy. This is again assumed to arise from the larger degree of ion scattering simulated for momentum exchange collisions with the “simple” model.

Finally, the effect of the Hall thruster exit plane profiles on the charge exchange plasma is shown in Fig. 18. The PIC-MCC profiles lead to an ion energy distribution that has the same peak as the baseline simulation, with a broader distribution that agrees more closely with the Express data.

Concluding Remarks

A hybrid particle-fluid PIC-DSMC model has been applied to model the plume of an SPT-100 Hall thruster operating under the same conditions experienced on the Russian Express satellites. Assessment of the model was performed through direct comparison of predictions with ion current density and ion energy distribution functions measured in orbit on the Express spacecraft. These data are the first to be taken in the plume of a Hall thruster operated in space. Comparison of the simulation predictions with the data therefore allowed many fundamental aspects of the plume model to be assessed in the space environment for the first time. Specifically, the following components of the model were assessed (the approach taken in the baseline simulation are indicated in parentheses): (1) the value of electron temperature assumed in the Boltzmann relation (3 eV); (2) the collision model (“detailed” model); and (3) the properties at the thruster exit plane (uniform profiles with an ion temperature of 4 eV).

In general, the comparisons indicated that the baseline plume model was able to capture most of the features found in the measured data. In terms of the ion current density profile, it was found from the simulation that the simple scaling law of $1/r^2$ for ion current density does not apply exactly as the plume

expands far away from the thruster. Agreement within a factor of two of most of the flight data was obtained at all angles for which data was measured. For the ion energy distribution measured in the primary ion beam, the baseline simulation again predicted the peak quite well, but the model distribution was significantly broader than the measured data. For the ion energy distribution measured in the charge exchange plasma, the baseline simulation correctly predicted the peak of the distribution, but provided a narrower profile and failed to simulate an extended high energy tail measured in space. For both ion energy distributions, a simulation performed using profiles at the thruster exit based on a separate PIC-MCC computation of the Hall thruster acceleration channel produced noticeably better results. It is therefore concluded that end-to-end simulations from inside the thruster to the plume far-field are needed for accurate analysis of spacecraft integration issues for thrusters for which no flight data exists.

Acknowledgments

This work was funded in part by the TRW Foundation. The author wishes to thank David Manzella for providing the Express data in electronic form.

References

- ¹ Boyd, I.D., "Review of Hall Thruster Plume Modeling," *Journal of Spacecraft and Rockets*, Vol. 38, 2001, pp. 381-387.
- ² Manzella, D. H., Jankovsky, R., Elliott, F., Mikellides, I., Jongeward, G., and Allen, D., "Hall Thruster Plume Measurements On-Board the Russian Express Satellites," IEPC Paper 2001-044, October 2001.
- ³ Myers, R. M. and Manzella, D. H., "Stationary Plasma Thruster Plume Characteristics," IEPC Paper 93-096, Sept. 1993.
- ⁴ Manzella, D. H. and Sankovic, J. M., "Hall Thruster Ion Beam Characterization," AIAA Paper 95-2927, July 1995.
- ⁵ Kim, S., Foster, J. E., and Gallimore, A. D., "Very Near-Field Plume Study of a 1.35 kW SPT-100," AIAA Paper 96-2972, July 1996.
- ⁶ King, L. B., "Transport-Property and Mass Spectral Measurements in the Plasma Exhaust Plume of a Hall-Effect Space Propulsion System," Doctoral Thesis, Department of Aerospace Engineering, University of Michigan, 1998.
- ⁷ Oh, D. Y., Hastings, D. E., Marrese, C. M., Haas, J. M., and Gallimore, A. D., "Modeling of Stationary Plasma Thruster-100 Thruster Plumes and Implications for Satellite Design," *Journal of Propulsion and Power*, Vol. 15., No. 2, 1999, pp. 345-357.
- ⁸ VanGilder, D. B., Boyd, I. D., and Keidar, M., "Particle Simulations of a Hall Thruster Plume," *Journal of Spacecraft and Rockets*, Vol. 37, No. 1, 2000, pp. 129-136.
- ⁹ Garrigues, L., Boyd, I. D., and Boeuf, J. P., "Computation of Hall Thruster Performance," *Journal of Propulsion and Power*, Vol. 17, 2001, pp. 772-779.
- ¹⁰ Birdsall, C. K. and Langdon, A. B., *Plasma Physics Via Computer Simulation*, Adam Hilger Press, 1991.

- ¹¹ Bird, G. A., *Molecular Gas Dynamics and the Direct Simulation of Gas Flows*, Oxford University Press, Oxford, 1994.
- ¹² Boyd, I. D., "Particle Simulation of an Anode Layer Hall Thruster Plume," *Journal of Propulsion and Power*, Vol. 16, No. 5, 2000, pp. 902-909.
- ¹³ Dalgarno, A., McDowell, M. R. C., and Williams, A., "The Mobilities of Ions in Unlike Gases," *Proceedings of the Royal Society*, Vol. 250, April 1958, pp. 411-425.
- ¹⁴ Miller, S., D. J. Levandier, Y. Chiu, and R. A. Dressler, "Xenon charge exchange cross sections for electrostatic thruster models," *Journal of Applied Physics*, in press, 2002.
- ¹⁵ Katz, I., G. Jongeward, V. Davis, M. Mandell, I. Mikellides, R. Dressler, I. Boyd, K. Kannenberg, J. Pollard, D. King, "A Hall effect thruster plume model including large-angle elastic scattering," AIAA Paper 2001-3355, July, 2001.
- ¹⁶ Boyd, I.D., Garrigues, L., Koo, J., and Keidar, M., "Progress in Development of a Combined Device/Plume Model for Hall Thrusters," AIAA Paper 00-3520, July 2000.
- ¹⁷ Perot, C., Gascon, N., Bechu, S., Lasgorceix, P., Dudeck, M., Garrigues, L. and Boeuf, J. P., "Characterization of a Laboratory Hall Thruster With Electrical Probes and Comparisons With a 2D Hybrid PIC-MCC Model," AIAA Paper 99-2716, June 1999.

Table 1. Properties at the exit of the SPT-100 Hall thruster.

Inner Diameter (mm)	60
Outer Diameter (mm)	100
Plasma Density (m^{-3})	10^{17} - 10^{18}
Neutral Density (m^{-3})	10^{18}
Ion Velocity (m/s)	17,000
Neutral Velocity (m/s)	300
Electron Temperature (eV)	4-10
Ion Temperature (eV)	1-4
Neutral Temperature (K)	1,000

Table 2. FWHM of ion energy distributions measured on centerline for SPT-100 thrusters.

Study	Instrument	FWHM (eV)	Angle (deg.)	Back Pressure (torr)
Myers & Manzella, Ref. 3	RPA	50	15	5×10^{-6}
King, Ref. 6	MBMS	40	0	4×10^{-5}
Perot et al., Ref. 17	RPA	39	0	2×10^{-5}
Express, Ref. 2	RPA	33	7.5	space

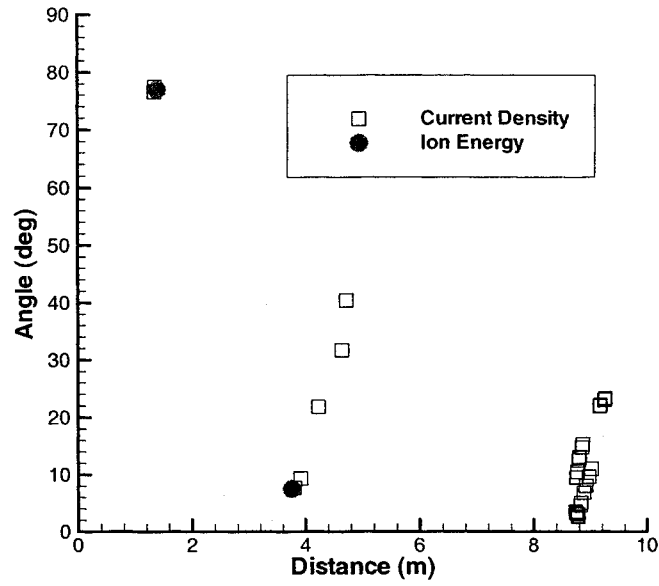


Fig. 1. Coordinates of the RPA sensors that provided the data employed in the present study.

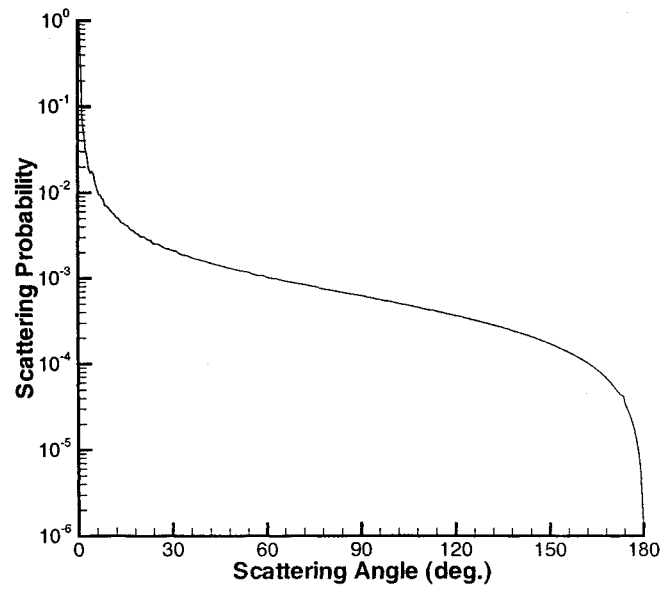


Fig. 2. Distribution of scattering angle for Xe-Xe⁺ interactions.

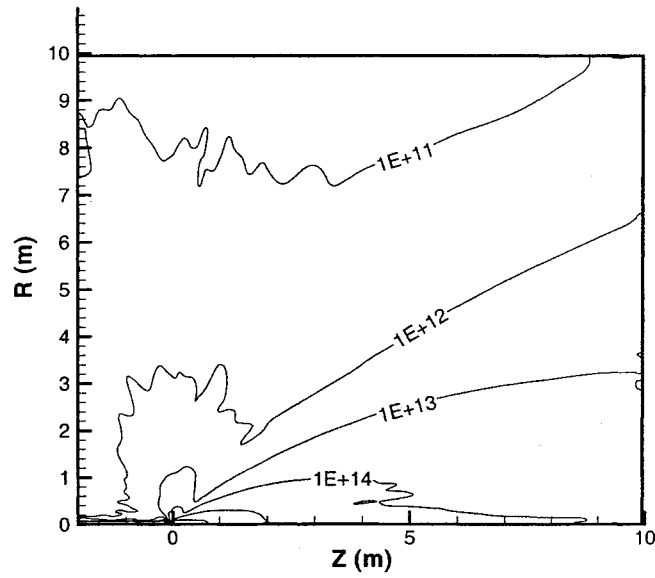


Fig. 3. Contours of ion number density (m^{-3}) for the baseline computation.

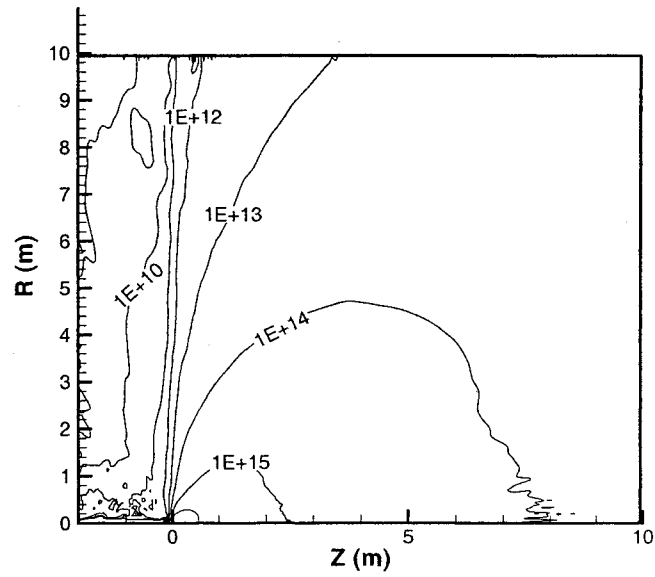


Fig. 4. Contours of neutral atom number density (m^{-3}) for the baseline computation.

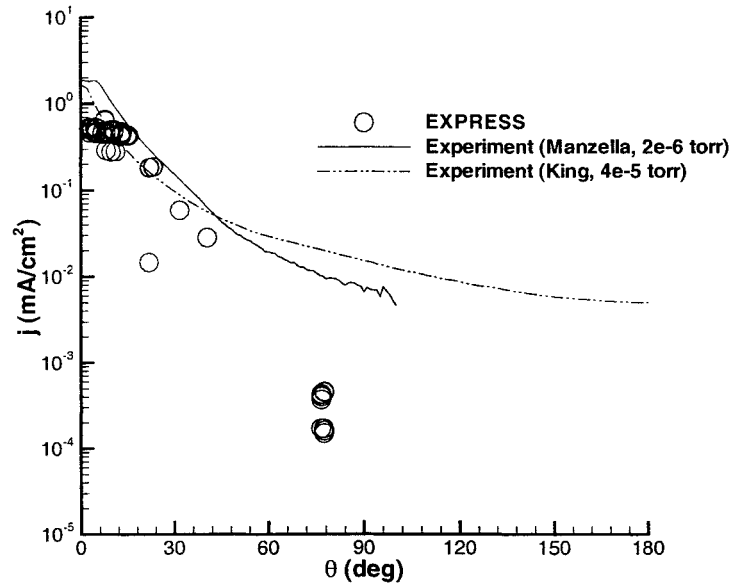


Fig. 5. Angular profiles of current density at 1 m from the thruster: comparison of flight and laboratory data.

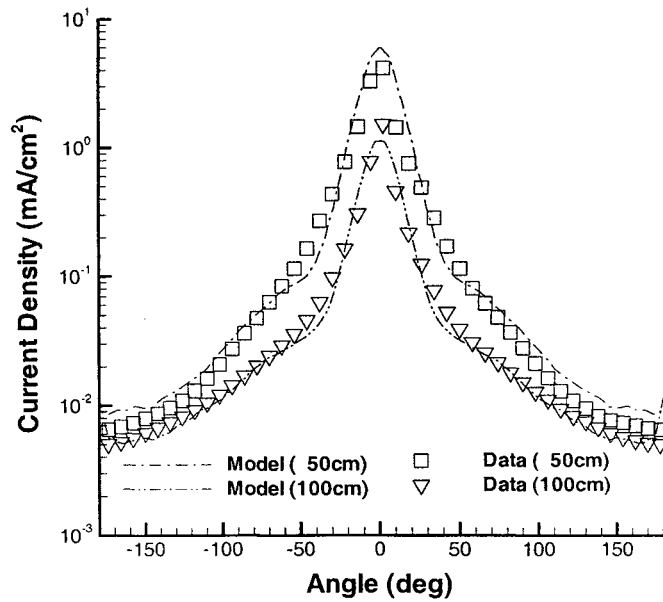


Fig. 6. Angular profiles of current density at 1 m from the thruster: comparison of model and laboratory data.

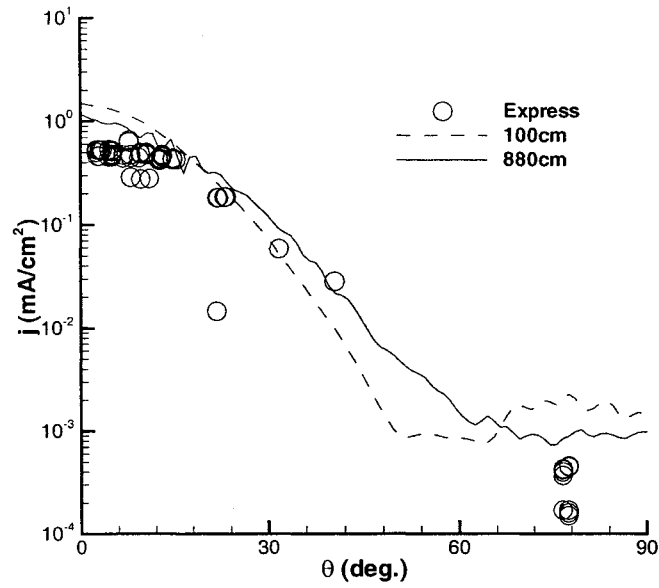


Fig. 7. Angular profiles of current density at 1 m from the thruster: comparison of model and flight data.

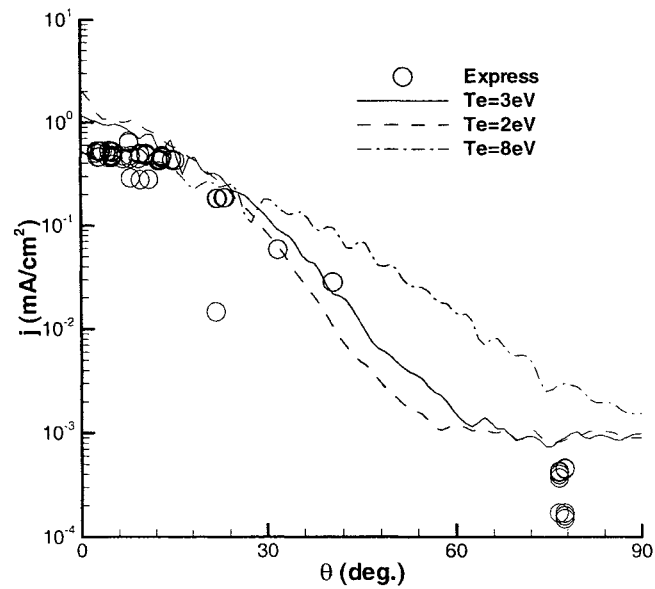


Fig. 8. Angular profiles of current density at 1 m from the thruster: effect of electron temperature.

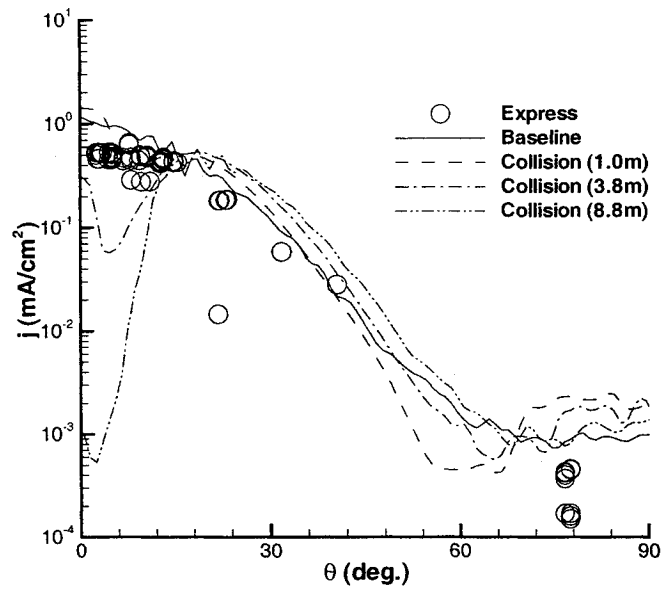


Fig. 9. Angular profiles of current density at 1 m from the thruster: effect of collision model.

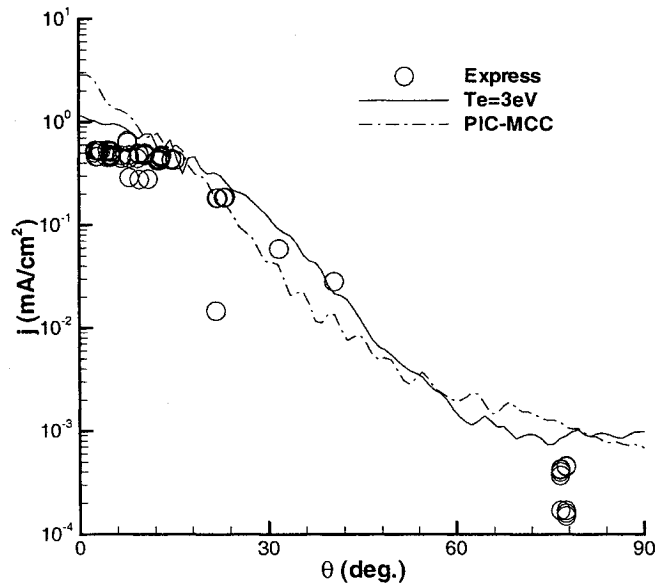


Fig. 10. Angular profiles of current density at 1 m from the thruster: effect of thruster exit profiles.

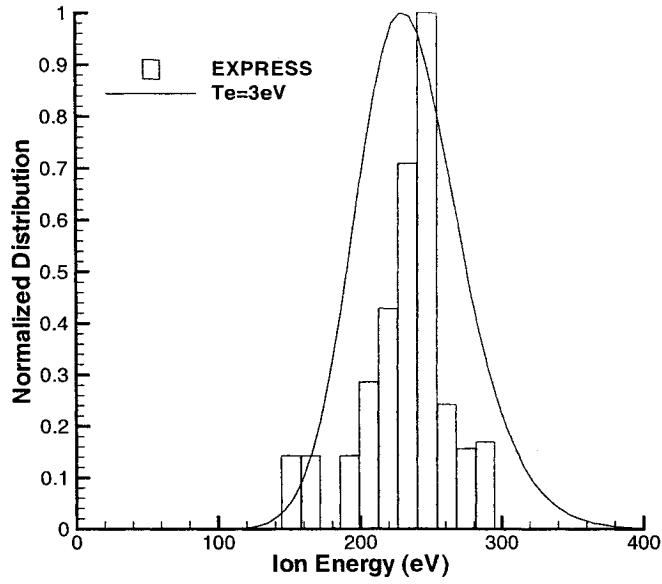


Fig. 11. Primary beam ion energy distribution function ($z=3.76$ m, $\theta=7.5^\circ$).

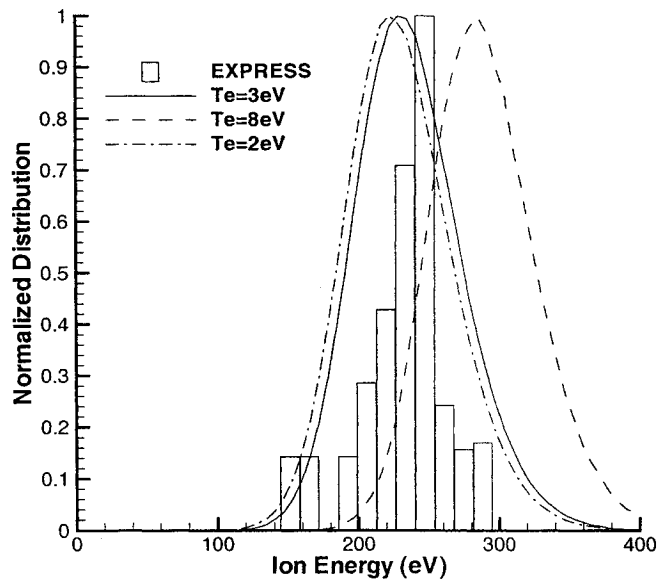


Fig. 12. Primary beam ion energy distribution function: effect of electron temperature.

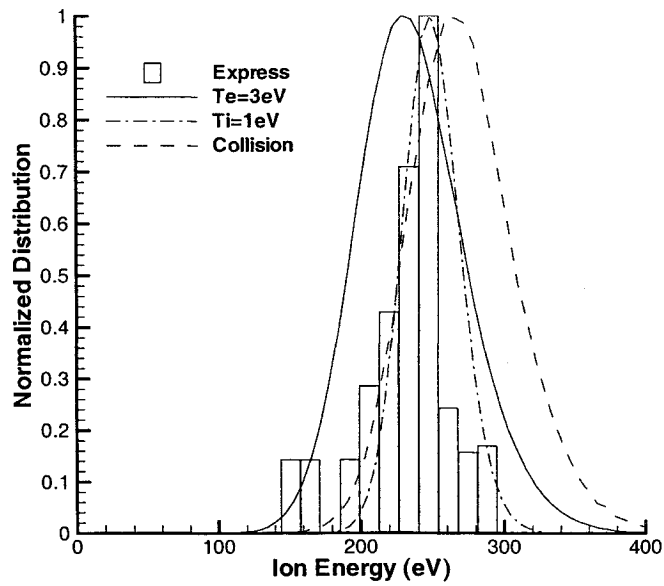


Fig. 13. Primary beam ion energy distribution function: effect of physical models.

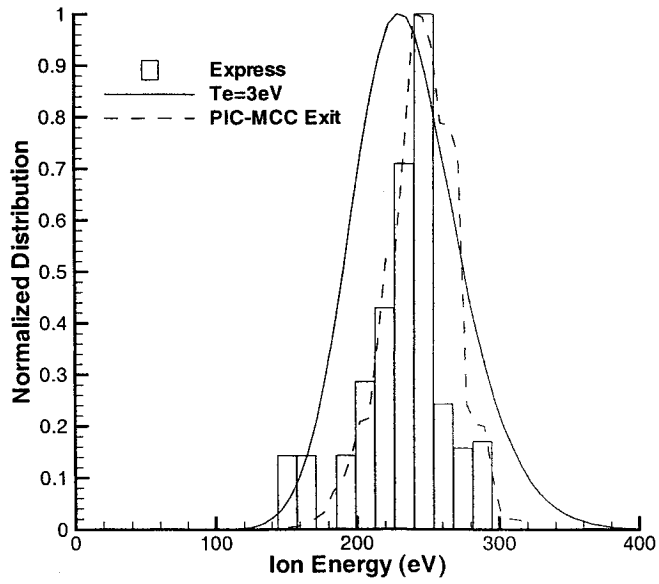


Fig. 14. Primary beam ion energy distribution function: effect of thruster exit profiles.

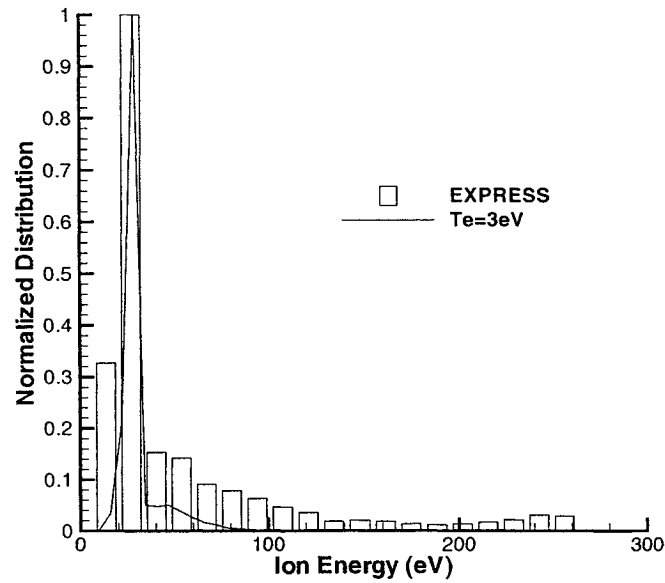


Fig. 15. Charge exchange ion energy distribution function ($z=1.40$ m, $\theta=77.5^\circ$).

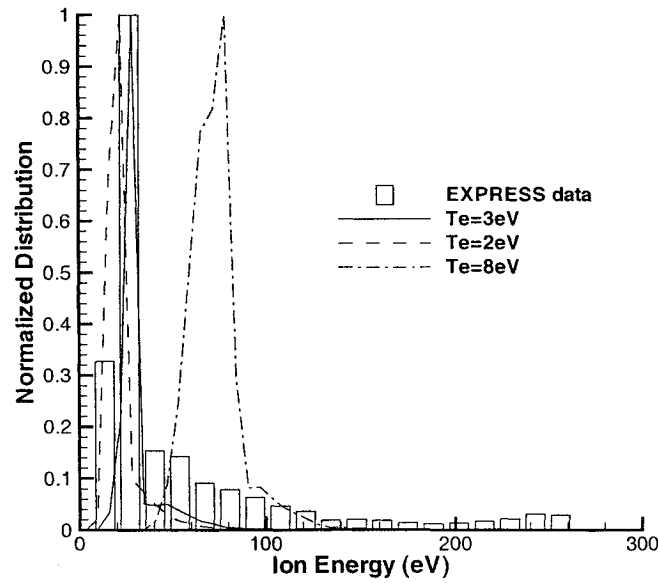


Fig. 16. Charge exchange ion energy distribution function: effect of electron temperature.

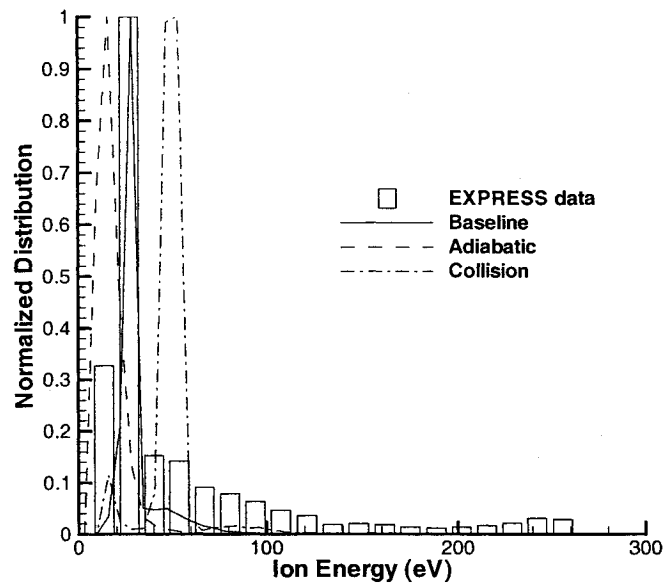


Fig. 17. Charge exchange ion energy distribution function: effect of physical models.

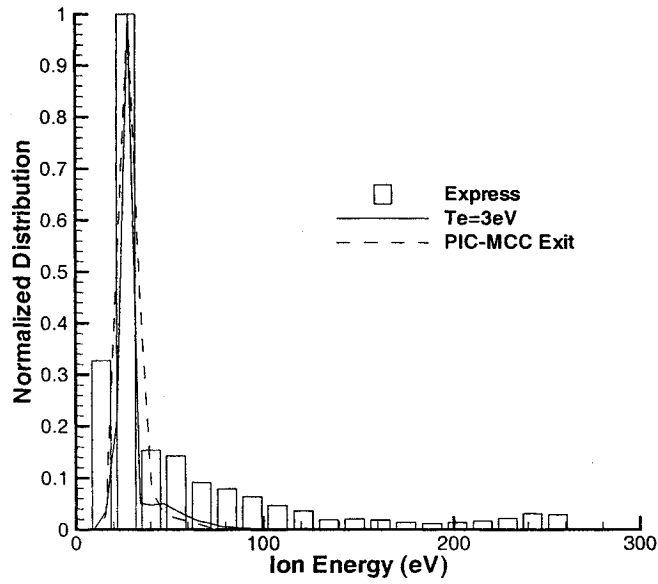


Fig. 18. Charge exchange ion energy distribution function: effect of thruster exit profiles.